Journal of Radioanalytical and Nuclear Chemistry (2024) 333:5335–5346
https://doi.org/10.1007/s10967-024-09618-z

Natural radiological risk assessment around archaeological sites, El-Dakhla Oasis (EDO), Egypt

Hesham M. H. Zakaly[1,2,3] · Reda Elsaman[1] · Mohamed Kamal[4,5] · Shams A. M. Issa[6] · Akbar Abbasi[7] · Jinsong Shen[4] · Atef El-Taher[1] · Chee Kong Yap[8] · Elsayed Abdelbaky[5] · El-Montser M. Seleem[5]

Received: 6 December 2023 / Accepted: 14 June 2024 / Published online: 10 July 2024

Abstract

The natural radionuclides in ancient El-Qasr village located in the El-Dakhla oasis (EDO), Egypt's Western Desert were measured using gamma-ray spectrometry equipped with a NaI (Tl) detector. The findings indicate that the samples' mean activity concentrations were 18.61 ± 1.02, 16.67 ± 0.9, and 137.67 ± 6.9 Bq kg^{-1} for ^{226}Ra, ^{232}Th, and ^{40}K, respectively. The values of Ra_{eq}, D, AED, H_{ex}, H_{in}, Iγ, and ELCR for the samples ranged anywhere from 34.1 to 83.9 Bq kg^{-1}, 15.7 to 37 nGy h^{-1}, 19.26 to 45.384 Sv y^{-1}, 0.09 to 0.23, 0.12 to 0.23, 0.25 to 0.59, and 6.74E−05 to 1.59E−04, respectively. These values are significantly lower than the international limit of 370 Bq kg^{-1} for Ra_{eq}, 59 nGy h^{-1} for D, 70 Sv y^{-1} for AED, 1 for H_{ex} and Hin, 2 for Iγ, and 29E−03 for ELCR. According to the obtained data, none of the samples seemed to be a significant risk when it came to radiation exposure. Using these data, we will determine the baseline level of radionuclides that occur naturally in the area that is the subject of the inquiry.

Keywords Baseline data · Radionuclide concentration · Radiation hazard

Introduction

The western desert of Egypt encompasses around 68% of the entire land area of the country. This region also contains the New Valley (NV) District and the Mediterranean coastal zone. The New Valley (NV) comprises the three oasis communities of Kharga, Dakhla, and Farafra. Dakhla is the largest oasis in the Western Desert and is located the farthest away from Egypt's major towns. It is believed that 75,000 people are living there among 17 separate villages. The Dakhla Oasis is composed of several minor oasis communities that are never very far from one another and are isolated from one another by either hills or deserts [1].

The primary problem under study is the potential radiological risk posed by naturally occurring radioactive materials (NORM) in the El-Dakhla Oasis region. The presence of radionuclides such as potassium, uranium, and thorium in the soil, rocks, and building materials can lead to long-term health hazards, particularly through inhalation and gamma radiation exposure[2–6].

Previous research has investigated the distribution of natural radionuclides in various regions globally. Studies have measured radionuclide concentrations in soil, water, and building materials to assess the associated health risks[7,

✉ Hesham M. H. Zakaly
h.m.zakaly@gmail.com; h.m.zakaly@azhar.edu.eg

✉ Akbar Abbasi
akbar.abbasi@kyrenia.edu.tr

1 Physics Department, Faculty of Science, Al-Azhar University, Assiut Branch, Assiut, Egypt

2 Faculty of Engineering and Natural Sciences, Istinye University, Istanbul 34396, Turkey

3 Institute of Physics and Technology, Ural Federal University, 620003 Ekaterinburg, Russia

4 China University of Petroleum, Beijing, China

5 Geology Department, Faculty of Science, Al-Azhar University, Assiut Branch, Assiut 71524, Egypt

6 Department of Physics, Faculty of Science, University of Tabuk, Tabuk, Saudi Arabia

7 Faculty of Art and Science, University of Kyrenia, TRNC, Via Mersin 10, Kyrenia, Turkey

8 Department of Biology, Faculty of Science, Universiti Putra Malaysia, 43400, UPM Serdang, Selangor, Malaysia

8]. However, there has been limited research specifically focused on the El-Dakhla Oasis, a region with significant archaeological and historical importance.

Brookes, 1993 states that only Mut and Qasr are considered to be towns among the 17 localities. The eastern region is dominated by the villages of Tenieda and Balat. The largest community in the oasis is Mut, which has 15,000 people living there. To the west of Mut are the settlements of Qasr and Mawhoub. Dakhla is situated at an elevation that is, on the whole, 122 m above the level of the mean sea. The lowest point of the Dakhla oasis may be found near Rashda, and it is around 88 m below sea level (a.m.s.l). After that, beginning in the southeast, the topography of the oasis begins to progressively ascend. The range of altitudes is from 110 to 140 m above mean sea level [9]. The natural radionuclides are present in trace amounts in all terrestrial formations, including rocks, soil, beach sand, sediments, and building materials, it is possible to locate radionuclides such as potassium, uranium, and thorium in these locations[10, 11]. Naturally occurring radioactive materials (NORM) such as ^{40}K and ^{238}U, ^{232}Th, and their decay products that are present in environmental materials such as soil [12–15], rock[6, 14], water [16–19], and building materials [20–24]. Because long-term exposure to uranium and radium occurs through inhalation, it is possible to understand these radioactive effects by studying the distribution of radionuclides. This is because the radioactive effects that result from exposure of the body and lung tissues to gamma rays and inhalation of radon gas are caused by radioactivity.

To address this gap, our study aimed to evaluate the natural radiation levels at the ancient sites within the El-Dakhla Oasis. We measured the concentrations of NORM, calculated various radiological risk indices such as radium equivalent activity (Ra_{eq}), absorbed dose rate (D), annual effective dose (AED), internal radiation hazard index (H_{in}), representative level index (I_r), and excess lifetime cancer risk (ELCR).

Understanding the levels of natural radionuclides in the region provides crucial insights for environmental pollution monitoring and assessing potential health risks. These findings are relevant to regulators and policymakers for establishing guidelines and safety measures to protect the local population and preserve the archaeological heritage of the El-Dakhla Oasis.

Cancer of the lung, pancreas, liver, and bones can result from exposure to thorium, according to research published by [25, 26]. Radium exposure can cause tumors in the bones and nose, while thorium exposure can cause cancer in those organs as well as the bones. Knowing the levels of natural radionuclides in the samples under investigation is significant, as it provides crucial insights into the monitoring of environmental pollution and the potential risks to human health arising from natural radioactivity. This is important because natural radioactivity can have a negative impact on human health.

This research was carried out to evaluate the concern of natural radiation of the ancient sites, in Egypt, and assessed the radiological risk indexes in the study area. For this purpose, the NORM concentration, radium equivalent activity (Ra_{eq}), absorbed dose rate (D), annual effective dose (AED), internal radiation hazard index (H_{in}), representative level index (I_r), and excess lifetime cancer risk (ELCR) were calculated in the study area.

Materials and methods

The geographical position of the study site

El-Qasr village is situated in the El-Dakhla oasis, located in the New Valley (NV) Governorate of Egypt. El-Dakhla is renowned as one of the oldest Islamic cities, serving as a crucial path for pilgrims and caravans travelling from the Maghreb en route to the Hijaz lands. The village is positioned 32 km north of the capital of El-Dakhla, Mutt. The El-Dakhla Oasis (EDO) is located approximately 120 kms west of the Kharga Oasis and around 300 kms west of the New Valley (NV). Furthermore, it lies approximately 300 kms southeast of the Farafra Oasis (as shown in Fig. 1). The geographic coordinates of El-Qasr village fall between latitudes 25°25′00″ and 25°45′00″N and longitudes 28°35′00″ and 29°15′00″ E (as illustrated in Fig. 2).

Accessibility

The Area under investigation is accessible through two roads. First, the northern part of the Area can be accessed through Through Cairo-Al-Wahat asphaltic road. Second, the eastern part of the Area can be accessed through the Assiut-El-Kharga Governorate asphaltic road, passing by El-Kharga and El-Dakhla oasis (EDO) (Fig. 1).

Physiography

The physiography of the study area was analyzed using a Digital Elevation Model (DEM) obtained from the Shouttle Radar Topography Mission (SRTM). This model was acquired from the United States Geological Survey (USGS)

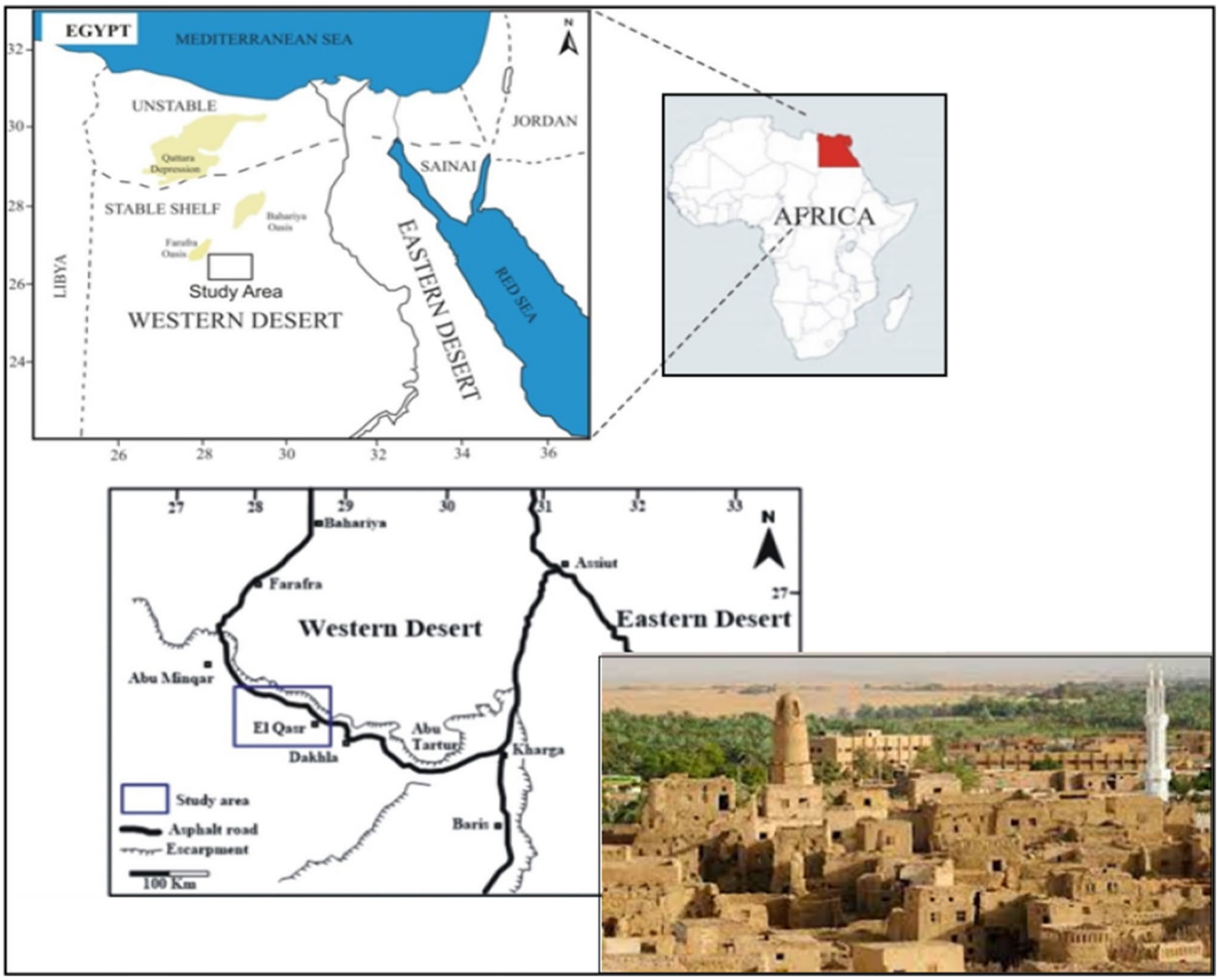

Fig. 1 displays a map indicating the geographical position of the area under investigation

website: http://earthexplorer.usgs.gov/. Additionally, a topographic contour map at a scale of 1:50,000 was published by the Egyptian Survey Authority in 1988 (as shown in Fig. 3). The analysis of these data sets reveals that the study area exhibits low to moderate topographical relief.

The importance of the study area

El-Qasr village is without a doubt one of the most crucial Islamic cities in the western Egypt and a main road to the Maghreb pilgrims' convoys (Fig. 4). The archaeological village of the El-Qasr includes ancient houses, and it contains the ruins of a mosque that date back to the first century after the common period, and it reaches its peak under the reign of the Ayyubids. The settlement served as both the oasis's city and the ruler's palace. There are several mosques from the Turkish and Mamluk eras; as well as a temple gate for the god Thoth. El-Qasr village isn't only a historical place, but it is an oasis for healing and treatment of diseases, especially rheumatic ones, as it is famous for its sulfur springs, especially with the availability of silt in the pools of these springs because of its therapeutic properties that cure many diseases.

Stratigraphy and structure of the study area

The Dakhla depression is characterized by a series of sedimentary formations that dip continuously with a slight inclination northward, resulting in large outcrops for each formation. The structures are typically not visible in the oasis depression but can be observed at the cliff to the north of the depression. The study area is dominated by late Mesozoic-early Cenozoic rocks that are separated into different

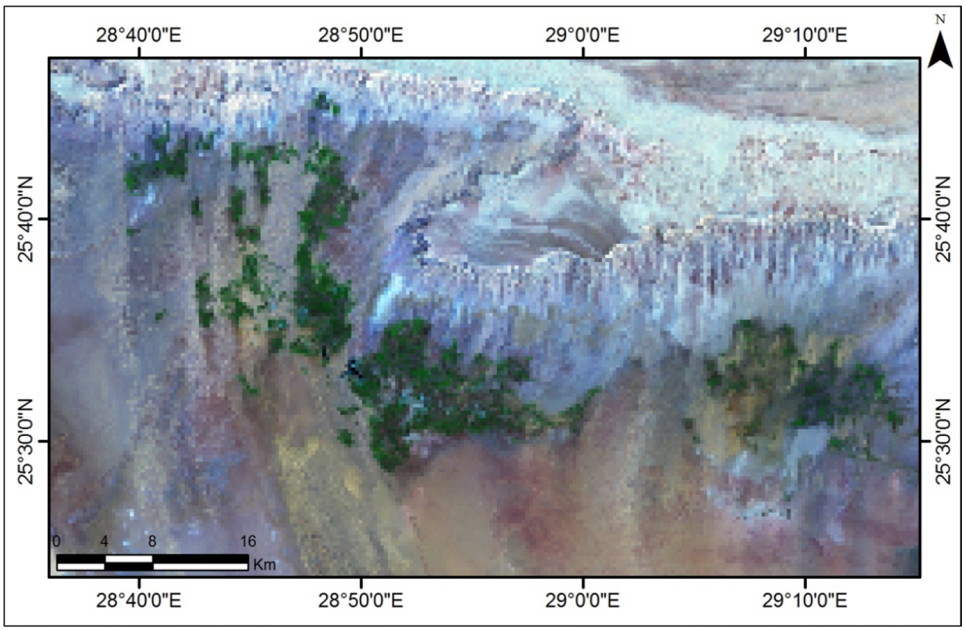

Fig. 2 The study area is depicted in the Landsat-8 (OLI) image

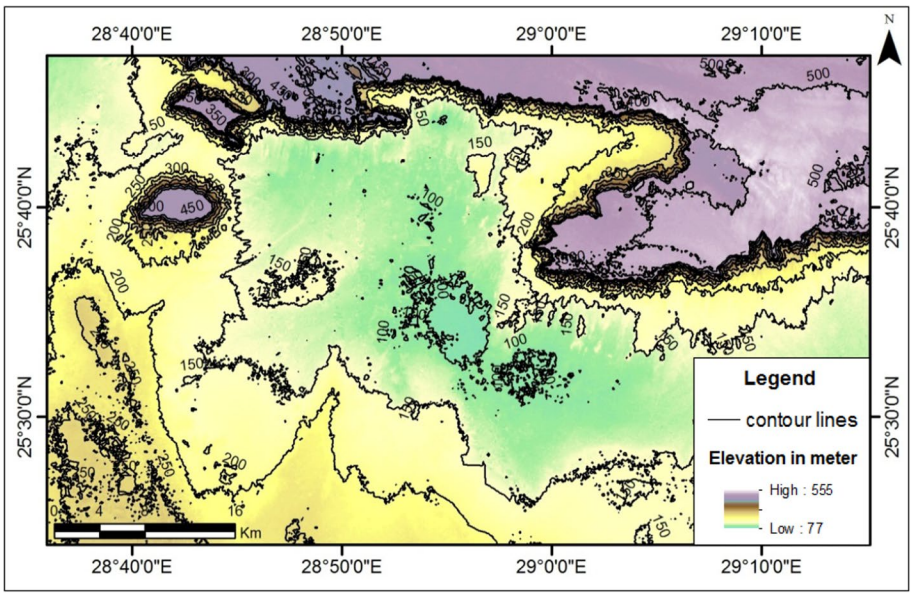

Fig. 3 Contour map showing the topography in the study area

mappable lithostratigraphic units. These units can be broadly classified into two groups: (a) a Campanian Lower Eocence (CLE) open-ocean Sequence of Transgression and Regression and (b) a Jurassic Campanian (JC) sequence that is primarily continental but has marine intercalations.

The Jurassic-Campanian sequence comprises sandstone and clay strata primarily from the continent and was previously referred to as the "Nubia Sandstone" formation. This sequence was deposited during a cyclic period of continental and marine deposition and includes the 6 Hills conglomeration (Late Jurassic- lower Cetaceous), the Sabaya Formation, and the Taref Formation, which were deposited in continental basins. The shallow marine deposits consist of the AB Formation (Aptian) and the Maghrabi Formation (Cenomanian) [27–29].

Massive aeolian accumulations may be discovered in the depression, and they are what constitute the quaternary sediments. The playas in the area are located between Tenieda and west of Mawhoub and consist of lacustrine playa deposits, which are arranged horizontally and alternately and contain bands of soft, friable sand, clay, and silt with plant

Fig. 4 displays photomicrographs that exhibit the study area's historical structures, namely (**A**) an old house, (**B**) a temple gate dedicated to the god Thoth, and (**C**) the remains of a mosque from the first century AH

remnants. Layers of salt crusts, caused by capillary rising groundwater, accumulate and intercalate with the lacustrine deposits in some locations [30–33]**.**

Generally, the structure of the area under examination lies inside the safe confines of the shelf that occupies the southern part of the Western Desert. It lies within the Dakhla Depression, which is considered a major plunging syncline which forms part of the regional Dakhla basin. The Dakhla syncline is thrown into several small anticline and synclinal undulations of different intensities, whose axis runs in a NE—SW direction and passes by Mut [34–36] considered the Dakhla depression as a structurally

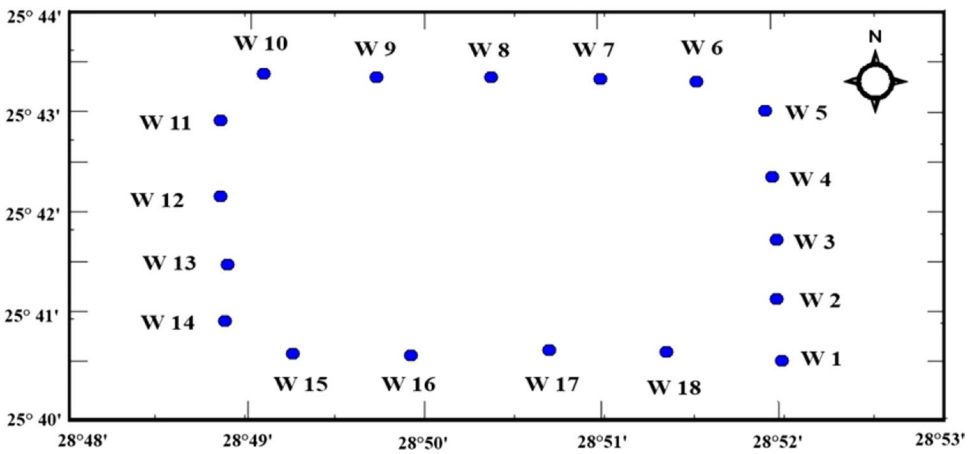

Fig. 5 Samples distribution in the studied Area

low area occurring between major structural highs. Generally, the Dakhla depression is considered a major broad syncline. This Dakhla major syncline is formed of small anticlines and synclines of different intensities. These anticlines are Bodkholou, Tawil and the Tartur highland, alternating with these are the synclines of El Mawhoub, Mut and Teneda.

Samples gathering and handling

A total of 18 samples were taken from El Qasr, which is an oasis in the Western Desert of Egypt (WDE) and is located in the El-Dakhla region. The number of samples was determined based on ensuring a representative distribution across the study area, considering various geographical and archaeological features. 10 samples were taken in the direction of the east and north. Eight samples were taken in the direction of the west and south (Fig. 5). The samples were oven-dried at 110° for twenty hours to guarantee that all traces of moisture were removed without altering the sample composition. This temperature is sufficient to evaporate water content while preserving the integrity of the samples. After placing the samples in beakers, the beakers were sealed entirely for 4 weeks, during which time the researchers waited for the samples to reach a state of secular equilibrium. This procedure is critical for assuring that the Rn-gas, as well as the daughters of the radon, will be confined inside the volume, according to the research carried out by [37].

Instrumentation and calibration

The radiation levels were determined with the use of a spectrometer that had a sodium iodide detector (NaI (Tl) 3 by 3 inches. The detection limit of the detector was established through repeated measurements of standard reference materials and background samples[38, 39]. To characterise the detector's surrounding background distribution, a counting procedure was performed on an empty, hermetically sealed beaker of the same shape and dimensions that were used for the samples. The lower detection limit was 2.4, 1.4, and 5.8 Bq kg^{-1} for ^{226}Ra, ^{232}Th, and ^{40}K, respectively., which ensures the accuracy and sensitivity required for our measurements [40]. In all, 43,200 s were spent determining whether the measurement was of the action or the background. The background spectra were used as a point of reference to adjust the area under the peak produced by the discovered isotopes. Finally, ^{40}K was evaluated from the 1461 keV peak of ^{40}K itself [25, 41, 42]. ^{226}Radium was computed from ^{214}Bi at energies of (609.3, 1120.3, and 1728.6 keV), and ^{214}Pb at 1764 keV. ^{232}Th was calculated at an energy of 911.2 keV from ^{228}Ac, and 238.6 keV from ^{212}P.

Table 1 The Specific activities of ^{226}Ra, ^{232}Th and ^{40}K present in the samples

Region name	Sample code	Activity ($BqKg^{-1}$)		
		^{226}Ra	^{232}Th	^{40}K
El Qasr (Dakhla oasis)	W-01	26 ± 1.3	15 ± 0.8	115 ± 5.7
	W-02	29 ± 1.4	21 ± 1.1	122 ± 6.1
	W-03	14 ± 0.7	18 ± 0.9	126 ± 6.3
	W-04	22 ± 1.1	15 ± 0.7	111 ± 5.6
	W-05	18 ± 0.9	15 ± 0.8	120 ± 6.0
	W-06	16 ± 0.8	8 ± 0.8	112 ± 5.6
	W-07	24 ± 1.2	17 ± 0.8	166 ± 8.3
	W-08	31 ± 3.1	31 ± 1.5	114 ± 5.7
	W-09	14 ± 0.7	23 ± 1.2	150 ± 7.5
	W-10	14 ± 0.7	23 ± 1.1	147 ± 7.3
	W-11	13 ± 0.7	15 ± 0.8	186 ± 9.3
	W-12	17 ± 0.9	17 ± 0.8	155 ± 7.7
	W-13	12 ± 0.6	13 ± 0.7	165 ± 8.2
	W-14	10 ± 0.5	11 ± 0.5	117 ± 5.9
	W-15	20 ± 1.0	12 ± 0.6	125 ± 6.3
	W-16	17 ± 0.8	20 ± 1.0	148 ± 7.4
	W-17	26 ± 1.3	8 ± 1.0	186 ± 9.3
	W-18	12 ± 0.6	18 ± 0.9	113 ± 5.7
Average		18.61 ± 1.02	16.67 ± 0.9	137.67 ± 6.9

Table 2 displays the mean levels of activity concentrations of ^{226}Ra, ^{232}Th and ^{40}K in soil samples that were studied, as well as in soil samples from other countries

Country	Activity (BqKg-1)			References
	^{226}Ra	^{232}Th	^{40}K	
Egypt [(El Qasr (Dakhla oasis)]	18.61 ± 1.02	16.67 ± 0.9	137.67 ± 6.9	This work
Siwa Oasis, Egypt	20.90 ± 1.80	17.70 ± 1.20	180 ± 10	[25]
Turkey	85.75	51.08	771.57	[44]
EL-Mynia, Egypt	21	12.10	154.40	[45]
Jordan	57.70	18.10	138.10	[46]
Algeria	53.20	50.03	311	[47]
Panama, Brazil	10.22	7.27	54.75	[48]
Jos Plateau, Niger	NM	734	115.80	[49]
India (Tamil Nadu)	–	27–794.3	44–251.4	[50]
Pakistan(Pakka Anna)	30–38	50–64	560–635	[51]
Sudan	11.6	6.02	158.4	[52]
Nigeria (Gombe state)	11.90	17.72	70.44	[53]
World average (soil)	33	45	420	[43]

NA not available

Results and discussion

Activity concentrations

Table 1 presents the activity concentrations of ^{226}Ra, ^{232}Th, and ^{40}K in the analysed soil samples. The mean and range of the activity concentrations (Bq kg^{-1}) in the samples were 18.61 ± 1.02 (10 ± 5.0–31 ± 3.1) for ^{226}Ra, 16.67 ± 0.9 (8 ± 1–31 ± 1.5) for ^{232}Th and 137.67 ± 6.9 (112 ± 5.6–186 ± 9.3) for ^{40}K. The (W8) sample has the maximum concentrations of ^{226}Ra (31 ± 3.1) and ^{232}Th (31 ± 1.5), while the (W14 and W17) samples have the lowest concentrations of radium-226 and thorium-232, respectively. The sample with the code W17 also had the greatest value of ^{40} K concentration, whereas the sample with the code had the lowest concentration (W6). The study found that the mean concentrations of ^{226}Ra, ^{232}Th, and ^{40} K in the soil samples collected were lower than the global average levels (33, 45, and 420) for ^{226}Ra, ^{232}Th, and ^{40}K respectively, as reported by UNSCEAR in 2008 [43]. Table 2 presents the analysis of the current study's soil samples about previous reports of the activity concentrations of these radionuclides. The results indicate that the concentrations of these radionuclides in the soil samples collected from Brazil were higher than those found in the other countries listed in the table. However, the mean values of ^{226}Ra, ^{232}Th, and ^{40}K in the soil samples collected in this study were lower than those found in Panama.

Radiation risk

The purpose of this study is to evaluate the radiation risk of the collected samples, several parameters were calculated. These include radium equivalent activity (Ra_{eq}), absorbed dose rate (D) in air, annual effective dose rate (AED), external hazard index (H_{ex}), internal hazard index (H_{in}), representative level index (I), and excess lifetime cancer risk (ELCR). The values for these parameters were determined using the equations presented in our previous works[8, 54–56], where A_{Ra}, A_{Th}, and A_K represent the activities of ^{226}Ra, ^{232}Th, and ^{40}K, respectively.

It is important to evaluate these parameters as they indicate the potential dangers to one's health from being exposed to the radiation levels present in the studied area. By computing these values, it can be determined whether the levels of radiation in the area are within acceptable limits or if there is a potential hazard to human health. The calculations show that the radiation hazard associated with the studied area is within safe limits, as the values of H_{ex}, H_{in}, and $I_{\gamma r}$ are less than 1. Moreover, the AED is lower than the recommended limit of 1 mSv per year for the general public. These findings suggest that the samples collected from the studied area are not a significant radiation hazard.

Table 2 contains the findings about the dangers posed by radioactive substances. As can be observed in Table 3, the values of Ra_{eq}, D, AED, H_{ex}, H_{in}, Ir, and ELCR for the samples ranged anywhere from 34.1 to 83.9 Bq kg^{-1}, 15.7 to 37

Table 3 The values for radium equivalent activity (Ra_{eq}), absorbed dose rate (D), annual effective dose (AED), internal radiation hazard index (H_{in}), representative level index (Ir), and excess lifetime cancer risk (ELCR)in study area

Region name	Sample code	Ra_{eq} ($BqKg^{-1}$)	Dose rate ($nGyh^{-1}$)	AED (μSvy^{-1})	Hazard indices			
					H_{ex}	H_{in}	Iγ	ELCR
El Qasr (Dakhla oasis)	W-01	56.8	25.7	31.55	0.15	0.23	0.40	1.10E−04
	W-02	68.4	30.6	37.58	0.19	0.26	0.48	1.32E−04
	W-03	48.8	22.0	26.98	0.13	0.17	0.35	9.44E−05
	W-04	51.4	23.3	28.54	0.14	0.20	0.37	9.99E−05
	W-05	49.0	22.2	27.23	0.13	0.18	0.35	9.53E−05
	W-06	39.1	18.0	22.11	0.11	0.15	0.26	7.74E−05
	W-07	61.0	27.9	34.263	0.17	0.23	0.44	1.20E−04
	W-08	83.9	37.0	45.384	0.23	0.23	0.59	1.59E−04
	W-09	59.0	26.5	32.439	0.16	0.23	0.43	1.14E−04
	W-10	57.6	25.8	31.677	0.16	0.23	0.42	1.11E−04
	W-11	49.4	22.9	28.095	0.13	0.23	0.37	9.83E−05
	W-12	52.7	24.1	29.528	0.14	0.19	0.38	1.03E−04
	W-13	43.6	20.2	29.528	0.12	0.19	0.32	1.03E−04
	W-14	34.1	15.7	19.261	0.09	0.12	0.25	6.74E−05
	W-15	47.3	21.7	26.606	0.13	0.18	0.34	9.31E−05
	W-16	56.8	25.7	31.489	0.15	0.20	0.41	1.10E−04
	W-17	62.0	28.6	35.129	0.17	0.24	0.38	1.23E−04
	W-18	46.2	20.7	29.528	0.13	0.19	0.33	1.03E−04
	Average	53.73	27.37	30.38	0.15	0.20	0.38	1.06E−04

$nGy\ h^{-1}$, 19.26 to 45.384 $Sv\ y^{-1}$, 0.09 to 0.23, 0.12 to 0.23, 0.25 to 0.59, and 6.74E-05 to 1.59E-04, respectively. These values are significantly lower than the international limit of 370 Bq kg^{-1} for Ra_{eq}, 59 $nGyh^{-1}$ for D, 70 Svy^{-1} for AED, 1 for H_{ex} and Hin, 2 for Iγ, and 29E-03 for ELCR [57–59]. Accordingly, there is no danger to the general public in the Area that is currently under study. Figure 6 illustrates the distribution of the radiation hazards that were caused by the samples that were taken from the study area, while the relative contributions to Ra_{eq}, D and AED, I_γ, H_{ex}, and H_{in}, respectively. The respective contributions of ^{226}Ra, ^{232}Th, and ^{40}K ranged from 23.96 to 50.23%, from 22.10 to 56.50%, and from 10.44 to 29.37%, respectively. In the majority of samples, ^{226}Ra and ^{232}Th are the primary donors to Ra_{eq}. The relative contributions of ^{226}Ra and ^{232}Th to the D and AED are significantly greater than the relative contribution of potassium. The contribution to Hex was made by ^{232}Th, which was followed by ^{226}Ra, which was followed by ^{40}K. Lastly, ^{226}Ra is the primary component that contributes to H_{in} in each soil sample.

Conclusion

Eighteen soil samples from the village of Al-Qasr were collected and processed for gamma-ray spectrometry measurements of the natural radioactivity caused by ^{226}Ra, ^{232}Th, and ^{40}K. Daily calibrations were used to make measurements, and each sample was measured several times. The mean and range of the activity concentrations ($Bqkg^{-1}$) in the samples were 18.61 ± 1.02 (10 ± 5.0–31 ± 3.1) for ^{226}Ra, 16.67 ± 0.9 (8 ± 1–31 ± 1.5) for ^{232}Th and 137.67 ± 6.9 (112 ± 5.6–186 ± 9.3) for ^{40}K. The study found that the mean concentrations of ^{226}Ra, ^{232}Th, and ^{40}K in the soil samples collected were lower than the global average levels (33, 54, and 420) for ^{226}Ra, ^{232}Th, and ^{40}K respectively, as reported by UNSCEAR in 2008. Based on the results obtained from the study, it can be concluded that the studied area has a lower radiation hazard compared to the world average. The concentrations of ^{226}Ra, ^{232}Th, and ^{40}K compared to levels reported for other nations, those discovered in the soil samples were much lower, except for Brazil. The calculated radiation hazard indices, such as the Ra_{eq}, D, AED, H_{ex}, H_{in}, I_γ, and

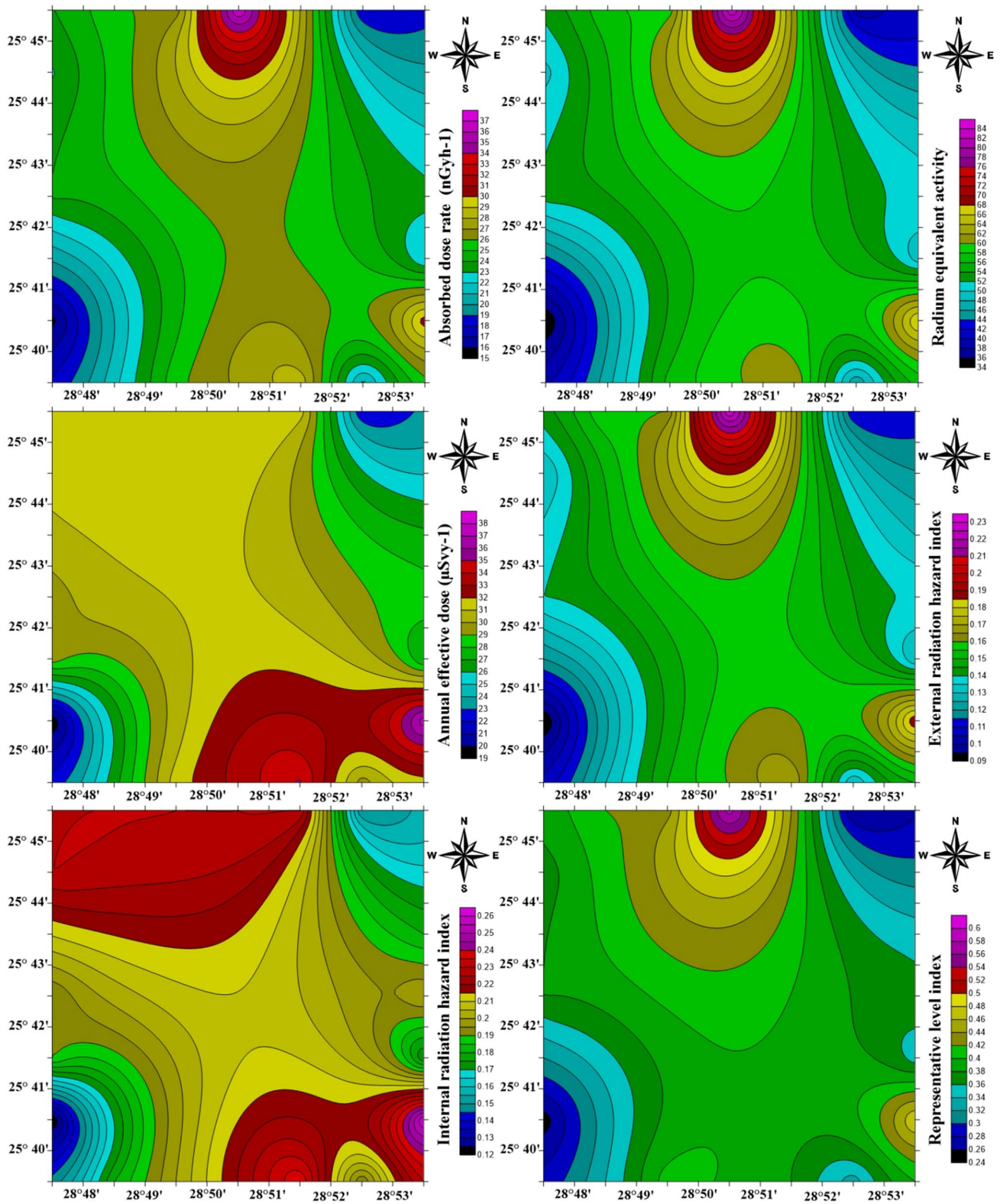

Fig. 6 The dispersion of radiation risks in the area under investigation

ELCR, were within safe limits (370 Bq kg^{-1}, 59 nGy h^{-1}, 70 Sv y^{-1}, 1, 2 and 29E-03 for Ra_{eq}, D, AED, H_{ex}, H_{in}, I_{γ}, and ELCR). However, it is important to continue monitoring radiation levels in the area to ensure the safety of the local population and the environment.

Acknowledgements The research partially funded by the Ministry of Science and Higher Education of the Russian Federation (Ural Federal University Program of Development within the Priority-2030 Program) is gratefully acknowledged. The authors express their gratitude to the University of Kyrenia and Al-Azhar University for their generous support.

Author contributions Hesham MH. Zakaly: Conceptualization, Writing- Original draft preparation, Methodology, Software. R. Elsaman: Writing- Original draft preparation, Supervision. Mohamed Kamal: Writing- Review& Editing, draft preparation. Shams A.M. Issa: Writing- Review& Editing, Methodology, Software, Project administration. Akbar Abbasi: Investigation, Conceptualization, Project administration, Visualization. Jinsong Shen: Methodology, Software. Atef El-Taher: Original draft preparation, Review& Editing. Chee Kong Yap: Investigation, original draft preparation. Elsayed Abdelbaky: Investigation, Methodology. El-Montser M. Seleem: Conceptualization, administration, Visualization.

Funding Open access funding provided by the Scientific and Technological Research Council of Türkiye (TÜBİTAK). Not applicable.

Data availability Data will be available upon request.

Declarations

Conflict of interest The authors declare that they have no known competing financial interests or personal relationships that could have appeared to influence the work reported in this paper.

References

1. Brookes IA (1993) Geomorphology and quaternary geology of the Dakhla Oasis Region, Egypt. Quat Sci Rev 12:529–552. https://doi.org/10.1016/0277-3791(93)90068-W
2. Tzortzis M, Tsertos H, Christofides S, Christodoulides G (2003) Gamma-ray measurements of naturally occurring radioactive samples from Cyprus characteristic geological rocks. Radiat Meas 37:221–229. https://doi.org/10.1016/S1350-4487(03)00028-3
3. Sonkawade RG, Kant K, Muralithar S et al (2008) Natural radioactivity in common building construction and radiation shielding materials. Atmos Environ 42:2254–2259. https://doi.org/10.1016/j.atmosenv.2007.11.037
4. Anjos RM, Veiga R, Soares T et al (2005) Natural radionuclide distribution in Brazilian commercial granites. Radiat Meas 39:245–253. https://doi.org/10.1016/j.radmeas.2004.05.002
5. Ghoneim MM, Panova EG, Abdel Gawad AE et al (2021) (2021) Analytical methodology for geochemical features and radioactive elements for intrusive rocks in El Sela area, Eastern Desert Egypt. Int J Environ Anal Chem. https://doi.org/10.1080/03067319.2021.1873310
6. Abed NS, Monsif MA, Zakaly HMH et al (2022) Assessing the radiological risks associated with high natural radioactivity of microgranitic rocks: a case study in a Northeastern Desert of Egypt. Int J Environ Res Public Health 19:473. https://doi.org/10.3390/IJERPH19010473
7. Tawfic AF, Zakaly HMH, Awad HA et al (2021) Natural radioactivity levels and radiological implications in the high natural radiation area of Wadi El Reddah, Egypt. J Radioanal Nucl Chem 327:643–652. https://doi.org/10.1007/s10967-020-07554-2
8. Zakaly HMH, Uosif MAM, Issa SAM et al (2021) An extended assessment of natural radioactivity in the sediments of the mid-region of the Egyptian Red Sea coast. Mar Pollut Bull 171:112658. https://doi.org/10.1016/j.marpolbul.2021.112658
9. Kleindienst MR, Churcher CS, McDonald MMA, Schwarcz HP (1999) Geography, geology, geochronology and geoarchaeology of the Dakhleh Oasis Region: an interim report. In: Reports from the Survey of the Dakhleh Oasis 1977–1987. pp 1–54
10. El-Taher A, Alshahri F, Elsaman R (2018) Environmental impacts of heavy metals, rare earth elements and natural radionuclides in marine sediment from Ras Tanura, Saudi Arabia along the Arabian Gulf. Appl Radiat Isot 132:95–104. https://doi.org/10.1016/j.apradiso.2017.11.022
11. Zakaly HM, Uosif MA, Madkour H et al (2019) Assessment of natural radionuclides and heavy metal concentrations in marine sediments in view of tourism activities in Hurghada city, northern Red Sea, Egypt. J Phys Sci 30:21–47. https://doi.org/10.21315/jps2019.30.3.3
12. Abbasi A, Mirekhtiary SF (2020) Radiological impacts in the high-level natural radiation exposure area residents in the Ramsar, Iran. Eur Phys J Plus. https://doi.org/10.1140/epjp/s13360-020-00306-x
13. Abbasi A (2019) Mirekhtiary SF (2019) Risk assessment due to various terrestrial radionuclides concentrations scenarios. Int J Radiat Biol. https://doi.org/10.1080/09553002.2019.1539881
14. Abbasi A (2023) Radiation risk assessment of coastal biota from a quasi-Fukushima hypothetical accident in the Mediterranean Sea. Mar Pollut Bull 194:115363. https://doi.org/10.1016/j.marpolbul.2023.115363
15. Abbasi A, Kurnaz A, Turhan Ş, Mirekhtiary F (2020) Radiation hazards and natural radioactivity levels in surface soil samples from dwelling areas of North Cyprus. J Radioanal Nucl Chem 324:203–210
16. Abbasi A, Mirekhtiary F (2019) Lifetime risk assessment of Radium-226 in drinking water samples. Int J Radiat Res. https://doi.org/10.18869/acadpub.ijrr.17.1.163
17. Abbasi A, Bashiry V (2016) Measurement of radium-226 concentration and dose calculation of drinking water samples in Guilan province of Iran. Int J Radiat Res. https://doi.org/10.18869/acadpub.ijrr.14.4.361
18. Abbasi A, Mirekhtiary F (2017) Gross alpha and beta exposure assessment due to intake of drinking water in Guilan, Iran. J Radioanal Nucl Chem. https://doi.org/10.1007/s10967-017-5493-6
19. Abbasi A, Almousa N, Zakaly HMH (2023) The distribution of radiotoxic 137Cs concentrations in seaweed and mussel species in

the Mediterranean Sea. Mar Pollut Bull 197:115737. https://doi.org/10.1016/j.marpolbul.2023.115737
20. Abbasi A (2017) Modeling of lung cancer risk due to radon exhalation of granite stone in dwelling houses. J Cancer Res Ther. https://doi.org/10.4103/0973-1482.204851
21. Abbasi A (2013) Calculation of gamma radiation dose rate and radon concentration due to granites used as building materials in Iran. Radiat Prot Dosim 155:335–342. https://doi.org/10.1093/rpd/nct003
22. Abbasi A, Mirekhtiary F (2013) Comparison ofactive and passive methods for radon exhalation from a high-exposure buildingmaterial. Radiat Prot Dosim 157:570–574. https://doi.org/10.1093/rpd/nct163
23. Abbasi A, Mirekhtiary F (2013) Comparison of active and passive methods for radon exhalation from a high–exposure building material. Radiat Prot Dosim 157:570–574
24. Abbasi A, Hassanzadeh M (2017) Measurement and Monte Carlo simulation of γ-ray dose rate in high-exposure building materials. Nucl Sci Tech. https://doi.org/10.1007/s41365-016-0171-x
25. Elsaman R, Seleem EMM, Salman SA et al (2022) Evaluation of natural radioactivity levels and associated radiological risk in soil from Siwa Oasis, Egypt. Radiochem 64:409–415. https://doi.org/10.1134/S1066362222030195
26. El-Taher A, Zakaly HMH, Elsaman R (2018) Environmental implications and spatial distribution of natural radionuclides and heavy metals in sediments from four harbours in the Egyptian Red Sea coast. Appl Radiat Isot 131:13–22. https://doi.org/10.1016/j.apradiso.2017.09.024
27. Farouk S, El-Desoky H, Heikal M et al (2020) Egyptian cretaceous clay deposits: insights on mineralogy, geochemistry, and industrial uses. Arab J Geosci 13:1–22. https://doi.org/10.1007/s12517-020-05557-7
28. Barthel KW, Boettcher R (1978) Abu Ballas Formation (Tithonian/Berriasian; Southwestern Desert, Egypt) a significant lithostratigraphic unit of the former "Nubian Series." Mitteilungen der Bayer Staatssammlung für Paläontologie und Hist Geol 18:153–166
29. Scheibner C, Speijer RP (2008) Late Paleocene-early Eocene Tethyan carbonate platform evolution - a response to long- and short-term paleoclimatic change. Earth-Sci Rev 90:71–102
30. El-Baz F, Maxwell TA (1982) Desert landforms of southwest Egypt: a basis for comparison with Mars
31. Maxwell TA (1982) Sand sheet and lag deposits in the southwestern desert. In: Desert landforms of southwest Egypt: a basis for comparison with mars. pp 157–173
32. Szabo BJ, Haynes CV, Maxwell TA (1995) Ages of Quaternary pluvial episodes determined by uranium-series and radiocarbon dating of lacustrine deposits of Eastern Sahara. "Palaeogeography. Palaeoclimatol Palaeoecol 113:227–242. https://doi.org/10.1016/0031-0182(95)00052-N
33. Pachur H-J (1999) 10 Paläo-Environment und Drainagesysteme der Ostsahara im Spätpleistozän und Holozän. Wiley
34. Embabi NS (2018) Geographic regions of Egypt. World geomorphological landscapes. Springer, Berlin, pp 3–13
35. Issawi B (1972) Review of upper cretaceous-lower tertiary stratigraphy in central and southern Egypt. Am Assoc Pet Geol Bull 56:1448–1463. https://doi.org/10.1306/819a40f2-16c5-11d7-8645000102c1865d
36. Lejal-Nicol A (2017) Fossil flora. The geology of Egypt. CRC Press, Boca Raton, pp 615–626
37. Elsaman R, Omer MAA, Seleem EMM, El-Taher A (2018) Natural radioactivity levels and radiological hazards in soil samples around Abu Karqas Sugar Factory. J Environ Sci Technol 11:28–38. https://doi.org/10.3923/jest.2018.28.38
38. Abbasi A, Algethami M, Bawazeer O, Zakaly HMH (2022) Distribution of natural and anthropogenic radionuclides and associated radiation indices in the Southwestern coastline of Caspian Sea. Mar Pollut Bull. https://doi.org/10.1016/j.marpolbul.2022.113593
39. Ene A, Pantelică A, Sloată F et al (2023) Gamma spectrometry analysis of natural and man-made radioactivity and assessment of radiological risk in soils around steel industry. Rom J Phys 68(7–8):803
40. Fathy D, Zakaly HMH, Lasheen ESR et al (2023) Assessing geochemical and natural radioactivity impacts of Hamadat phosphatic mine through radiological indices. PLoS ONE 18:e0287422. https://doi.org/10.1371/JOURNAL.PONE.0287422
41. Ghoneim MM, Abdel Gawad AE, Awad HA et al (2021) Distribution patterns of natural radioactivity and rare earth elements in intrusive rocks (El Sela area, Eastern Desert, Egypt). Int J Environ Anal Chem. https://doi.org/10.1080/03067319.2021.1916006
42. Zakaly HMH, Abbasi A, Almousa N, Savaşan A (2024) Naturally occurring radioactive materials (NORM) concentration and health risk assessment of aerosols dust in Nicosia, North Cyprus. J Radioanal Nucl Chem 333:1073–1082. https://doi.org/10.1007/s10967-023-09346-w
43. UNSCEAR United Nations Scientific Comittee on the Effects of Atomic Radiation (2000) Sources and effects of ionizing radiation. Annex B. Exposures of the public and workers from various sources of radiation
44. Dizman S, Görür FK, Keser R (2016) Determination of radioactivity levels of soil samples and the excess of lifetime cancer risk in Rize province, Turkey. Int J Radiat Res 14:237–244. https://doi.org/10.18869/acadpub.ijrr.14.3.237
45. Mostafa AMA, Uosif MAM, Elsaman R, Moustafa E (2016) Transmission of natural radiation from soil to maize plants and radiological hazards resulting from consumption in upper Egypt. J Phys Sci 27:25–49. https://doi.org/10.21315/jps2016.27.3.3
46. Saleh H, Abu Shayeb M (2014) Natural radioactivity distribution of southern part of Jordan (Ma′an) Soil. Ann Nucl Energy 65:184–189. https://doi.org/10.1016/j.anucene.2013.10.042
47. Boukhenfouf W, Boucenna A (2011) The radioactivity measurements in soils and fertilizers using gamma spectrometry technique. J Environ Radioact 102:336–339. https://doi.org/10.1016/j.jenvrad.2011.01.006
48. Becegato VA, Ferreira FJF, Machado WCP (2008) Concentration of radioactive elements (U, Th and K) derived from phosphatic fertilizers in cultivated soils. Braz Arch Biol Technol 51:1255–1266. https://doi.org/10.1590/S1516-89132008000600022
49. Jibiri NN, Farai IP, Alausa SK (2007) Estimation of annual effective dose due to natural radioactive elements in ingestion of foodstuffs in tin mining area of Jos-Plateau, Nigeria. J Environ Radioact 94:31–40. https://doi.org/10.1016/j.jenvrad.2006.12.011
50. Ajithra AK, Venkatraman B, Jose MT, Chandrasekar S, Shanthi G (2017) Assessment of natural radioactivity and associated radiation indices in soil samples from the high background radiation area, Kanyakumari district, Tamil Nadu India. Radiat Protect Environ 40(1):27–33
51. Akhtar N, Tufail M, Ashraf M et al (2005) Measurement of environmental radioactivity for estimation of radiation exposure from saline soil of Lahore, Pakistan. Radiat Meas 39:11–14. https://doi.org/10.1016/j.radmeas.2004.02.016
52. Sam AK, Ahamed MMO, El Khangi FA et al (1998) Radioactivity levels in the Red Sea coastal environment of Sudan. Mar Pollut Bull 36:19–26. https://doi.org/10.1016/S0025-326X(98)90025-X

53. Kolo M, Amin Y, Khandaker M, Abdullah W (2017) Radionuclide concentrations and excess lifetime cancer risk due to gamma radioactivity in tailing enriched soil around Maiganga coal mine, Northeast Nigeria
54. Abbasi A, Zakaly HMH, Mirekhtiary F (2020) Baseline levels of natural radionuclides concentration in sediments East coastline of North Cyprus. Mar Pollut Bull. https://doi.org/10.1016/j.marpolbul.2020.111793
55. Saudi HA, Abedelkader HT, Issa SAM et al (2022) An in-depth examination of the natural radiation and radioactive dangers associated with regularly used medicinal herbs. Int J Environ Res Public Heal 19:8124. https://doi.org/10.3390/IJERPH19138124
56. Moghazy NM, El-Tohamy AM, Fawzy MM et al (2021) Natural radioactivity, radiological hazard and petrographical studies on aswan granites used as building materials in Egypt. Appl Sci 11:6471. https://doi.org/10.3390/app11146471
57. Beretka J, Mathew PJ (1985) Natural radioactivity of australian building materials, industrial wastes and by-products. Health Phys 48:87–95. https://doi.org/10.1097/00004032-198501000-00007
58. Palomo M, Peñalver A, Aguilar C, Borrull F (2010) Presence of naturally occurring radioactive materials in sludge samples from several Spanish water treatment plants. J Hazard Mater 181:716–721. https://doi.org/10.1016/j.jhazmat.2010.05.071
59. Alaei P (2008) Introduction to health physics: fourth edition. Med Phys 35:5959. https://doi.org/10.1118/1.3021454